The Egyptian Journal of Radiology and Nuclear Medicine (2013) **44**, 737–746

Egyptian Society of Radiology and Nuclear Medicine

The Egyptian Journal of Radiology and Nuclear Medicine

www.elsevier.com/locate/ejrnm
www.sciencedirect.com

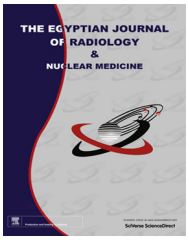

ORIGINAL ARTICLE

Role of dynamic contrast-enhanced and diffusion weighted MRI in evaluation of necrosis of hepatocellular carcinoma after chemoembolization

Reham M. Osama [a,*], Ahmed H.K. Abdelmaksoud [a], Sanaa A.M. El Tatawy [a], Mohammed M. Nabeel [b], Lamia I.A. Metwally [a]

[a] *Department of Radiology, Faculty of Medicine, Cairo University, Egypt*
[b] *Department of Endemic Medicine and Hepatology, Faculty of Medicine, Cairo University, Egypt*

Received 17 June 2013; accepted 25 September 2013
Available online 23 October 2013

KEYWORDS

Dynamic MRI;
Diffusion-weighted;
TACE;
Hepatocellular carcinoma

Abstract *Purpose:* The purpose of this study is to evaluate the role of dynamic contrast enhanced and diffusion weighted MRI in the assessment of response and necrosis in the treatment of hepatocelluar carcinoma after transcatheter arterial chemoembolization (TACE).
Subjects and methods: Precontrast T1, T2, STIR, Dynamic contrast enhanced and respiratory triggered diffusion weighted MR images (*b* factor, 500, 1000 s/mm^2 obtained in 50 patients with hepatocellular carcinoma who underwent transarterial hepatic chemoembolization). Diffusion-weighted MR images, gadolinium-enhanced MR images after TACE were assigned confidence levels for postoperative HCC recurrence. The sensitivity, specificity, PPV, NPV and overall agreement were cal-

Abbreviations: TACE, transarterial chemoembolization; CT, computed tomography; RECIST, response evaluation criteria in solid tumors; DCE MRI, dynamic contrast enhanced magnetic resonance imaging; ADC, apparent diffusion coefficient; THRIVE, high resolution isotropic volume examination; DWI, diffusion weighted imaging; GRAPPA, parallel imaging with generalized auto- calibrating partially parallel acquisition; ROI, region of interest; TSE, turbo spine echo; FFE, fast field echo.

* Corresponding author. Tel.: +20 1006886270.
E-mail address: reham81_2006@hotmail.com (R.M. Osama).

Peer review under responsibility of Egyptian Society of Radiology and Nuclear Medicine.

Production and hosting by Elsevier

 http://dx.doi.org/10.1016/j.ejrnm.2013.09.012

culated for both the dynamic and the DWI images. Apparent diffusion coefficients (ADCs) were calculated searching for a cut off value using the ROC curve.

Results: Dynamic MRI had a sensitivity of 90.5%, a specificity of 96.6%, a positive predictive value of 95%, a negative predictive value of 93.3% and an overall agreement of 94% compared to 100%, 65.5%, 67.7%, 100% and 80% respectively of diffusion weighted imaging.

The difference between the malignant and benign groups' ADC variables was statistically significant *P* value 0.006.

The ROC curve showed that the area under the curve is $C = 0.728$ with SE = 0.075 and 95% CI from 0.582 to 0.874.

Conclusion: Diffusion weighted MR imaging has lower specificity compared to dynamic MRI with increased false positives. We suggest that increase is due to intralesional hemorrhage or liquefactive necrosis causing diffusion restriction. Diffusion weighted imaging may act as a supplementary sequence to compensate the dynamic MRI in patients who could not hold their breath adequately.

1. Introduction

With the expanded use of locoregional therapies as a cornerstone in the treatment of tumors of multiple organs, it became indispensible to implement new radiological techniques to provide patients with more efficient follow up.

TACE affects the tumor to the maximum impact of chemotherapy by selective or superselective injection of tumor vessels by chemotherapeutic agents and reducing the tumoral blood flow by the embolization of particles resulting in prolonged contact of the tumor with the chemotherapeutic agents (1). Lipiodol is used as a carrier for the chemotherapeutic agents. It slowly reaches the sinusoids and then gets trapped within the tumor vessels that lack kupffer cells (2).

CT is still the examination of choice to follow up patients being performed immediately after the TACE procedure to ensure the retention of lipiodol by the tumor. It is repeated 1 month later for the detection of any tumoral residue or recurrence.

A diagnostic dilemma due to defective accumulation of lipidol either due to necrotic areas or residual tumor is still faced by radiologists. Also the hyperattenuating retained lipidol causes hardening artifact which degrades the interpretation of images (Fig. 1) (3).

Standardized criteria (RECIST) were still defective for monitoring the response to therapy, and this is attributed to the fact that such treatments may not lead to early regression of tumor volume, but rather an increase in the extent of tumor necrosis (4).

Takayasu et al. (5) concluded in their study that there is no correlation between tumor size reduction and the histopathologic necrosis rate in the resected specimens. Such a study explains the lack of this correlation by the delayed resorption of necrosis when the artery and sinusoid feeding the tumor are completely embolized and occluded.

Therefore, it has been recommended to modify the RECIST criteria to take into account only the diameters of the viable areas of the target lesions (i.e., the regions of tumors showing contrast enhancement during the arterial phase). However, the accurate measurement of lesion size is still difficult due to the wide variations between interpreters in estimating the position of the lesion edges. This is crucial especially in infiltrating tumors, in tumors containing irregular areas of necrosis or when small satellite lesions are surrounding the main tumor (4).

Besides, the surrounding post-treatment edematous changes could give rise to an apparent increase in size. Thus, change in tumor volume is not an indicator to predict the histological tumor response (6).

MRI allows the detection of anatomic, functional and molecular parameters in order to assess the response to treatment. Non-contrast T1- and T2-weighted images provide information concerning the morphological changes, changes in the fluid content and fibrosis. As for the dynamic contrast enhanced MRI (DCE MRI), it provides information regarding the tumoral perfusion (7). Contrast-enhanced MRI is sensitive to therapy-related changes in blood volume and vascular permeability which may be associated with tumor angiogenesis (8).

Diffusion weighted image provides an insight about water composition within a tumor and assessing the degree of tumor viability. The viable tumor cells have intact membranes that cause restricted water diffusion whereas necrotic tumors have increased water diffusion due to cell membrane disruption (9).

The apparent diffusion coefficient (ADC) calculated in diffusion-weighted MRI has become a good aiding biomarker of tumor response to therapy. The ADC is a measure of the mobility of water within tissues. The viable tumors are highly cellular, and the cells have an intact cell membrane that restricts the mobility of the water molecule resulting in a relatively low ADC. Conversely, the cellular necrosis increases membrane permeability, allowing free mobility of water molecules and causing an increase in ADC (10).

2. Subjects and methods

2.1. Patients

This study included 50 cases of HCC who underwent TACE. The study was conducted in the Kasr Al-Ainy Hospital. The patients were referred from the Tropical Department to the Radiology Department over a period of 18 months (June 2011–December 2012).The patients' age ranged from 40 to 79 years (median 60);42 patients were males and 8 were females. All patients had liver cirrhosis related to chronic viral hepatitis.

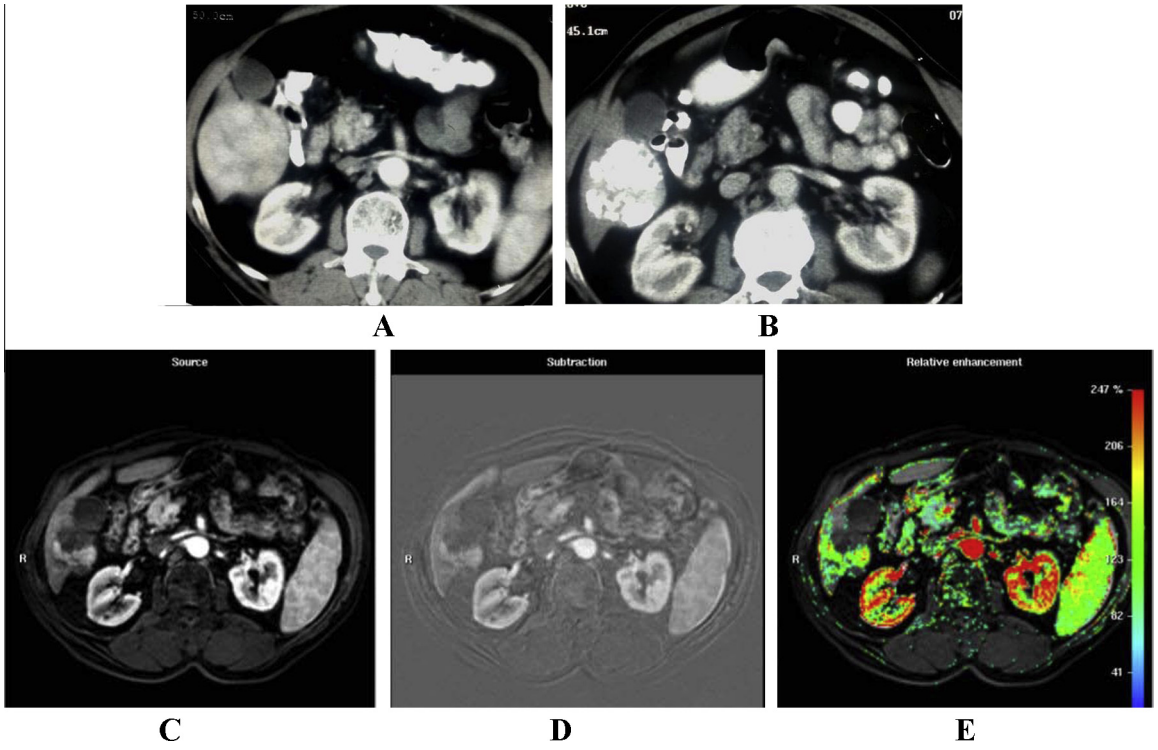

Fig. 1 The effect of hardening artifact on the interpretation of CT findings. (A) arterial phase contrast enhanced CT of a 60 year old male showing a well defined right hepatic lobe (segment VI) heterogenously enhancing mosaic HCC. (B) Post TACE arterial phase contrast enhanced CT of the same patient showing type II lipidol accumulation within the tumor; partial defect in the tumor; with difficulty to detect residual enhancing portions due to hardening artifact. (C–E) Dynamic MRI of the same patient (C) Early arterial phase of T1 THRIVE (High Resolution Isotropic Volume Examination), (D) Corresponding subtraction image and (E) Corresponding relative enhancement color mapping image. They show clearly the residual enhancing portions without being affected by the lipiodol signal.

2.1.1. TACE

All patients were examined in our multidisciplinary clinic. The procedure started by the Siledenger technique through the right femoral artery followed by catheterization of the common and proper hepatic arteries. Super-selective catheterization of the feeding artery was done in most of the cases using a micro-catheter then an injection of a mixture of Lipiodol and Adriamycin was injected.

2.1.2. MRI

MRI was performed using 1.5-T MRI scanner (Philips Intera) equipped with phased-array torso surface coil.

- Examination included precontrast axial T1, T2 and SPIR weighted images, coronal T1 and T2, dynamic and Diffusion MRI.
- Dynamic study was performed after bolus injection of 0.1 mmol/kg body weight of Gd-DTPA at a rate of 2 ml/s, flushed with 20 ml of sterile saline solution via the antecubital vein. The injection of contrast medium and saline solution was performed manually.
- Dynamic imaging using T1 THRIVE (High Resolution Isotropic Volume Examination) technique was performed in triphasic way; A dynamic series consisted of one pre contrast series followed by four successive post contrast series including early arterial, late arterial, and portal phase imaging with 18–21 s intervals (including 17–20 s for image acquisition with breath-holding according to liver size and 1 s for re-breathing for the start of each phase imaging) followed by 5-min delayed phase imaging. Image acquisition starts after contrast injection by 10 s. All patients were imaged in end expiration to limit the risk of image misregistration.
- DWI was performed before the dynamic imaging using respiratory triggered fat suppressed single-shot echoplanar sequence that combined the two diffusion (motion-probing) gradients before and after the 180° pulse along the three directions of section-select, phase-encoding, and frequency-encoding and data acquisition with EPI readout. It was obtained by applying three different b factors of 0, 500, and 1000 s/mm^2.
- Parallel imaging with generalized auto- calibrating partially parallel acquisition (GRAPPA) with an acceleration factor of two was applied to reduce the acquisition time.

2.2. MR images were analyzed for the following

1. Size and border of the lesion.
2. The T1, T2 and FAT SATURATED signal characteristics.
3. Pattern of enhancement in the dynamic imaging, subtracted images, and color mapping. For interpretation of the dynamic imaging, arterial hypervascularity and subsequent washout appearance were regarded as suggestive findings of

viable HCC. Meanwhile benign conditions were considered when progressive or persistent enhancement was detected on dynamic images.

4. Signal intensity on diffusion images with ADC values and fusion images using a commercially windows workstation (PHILIPS).The pattern of diffusion restriction was classified into- heterogeneous, rim and focal nodular.

- All DWI images using different b values were sorted for the confidence levels according to three grade scales:-
  (1) Benign conditions were considered when lost signal on diffusion images or mild sustained hyperintensity with bright ADC map (shine through effect) is noted.
  (2) Uncertainty is considered when sustained faint or moderate hyperintensity is seen on diffusion images with isointensity on ADC maps.
  (3) Viable tumor portion was identified by sustained hyperintensity in the diffusion images compared with the signal drop of background parenchyma with increasing *b* values combined with low ADC map.
- Intensity on diffusion images was classified mild-moderate-marked compared to the spinal cord on *b* value 1000.

2.3. ADC measurement

- Pixel-based ADC maps were generated on the workstation. ADC was calculated with linear regression analysis of the function $S = S0 \times \exp(-b \times \mathrm{ADC})$, where S is the signal intensity after application of the diffusion gradient, and $S0$ is the signal intensity at a b value of 0 s/mm^2. The three b values (0, 500, and 1000 s/mm^2) were used for ADC calculation.
- For precise placement of circular ROI in the small lesions, the center of the lesion on the DWI was determined by the interfacing point of two lines met at right angles which are a vertical line and a horizontal line from the upper and the left border of the images, respectively. With the knowledge of the length of each line, the identical lines could be drawn on the corresponding ADC map. With the reference of the lesion size on DWI, circular ROI was placed around the center point to measure the ADC of the lesion.
- A region of interest was drawn over any sustained hyperintensity areas on diffusion images, and if no high signal could be identified, the whole lesion was measured. The ADC was measured three times and the three measurements were averaged.

2.4. Statistical analysis

- Computer software package SPSS version 15 was used in the analysis.
- For quantitative variables, mean (as a measure of central tendency), and standard deviation (as measures of variability) were presented.
- Frequency and percentages were presented for qualitative variables.
- Chi-Square test was used to estimate differences in qualitative variables.
- A ROC (Receiver Operating Characteristic) curve was constructed and the area below the ROC curve was used to represent prediction precision.
- *P*-values less than 0.05 were considered as statistically significant.

2.5. The standard of reference

- It was difficult to obtain pathologic confirmation in patients who underwent chemoembolization because most of these patients do not undergo surgery. In addition, biopsy may result in sampling error.
- Residual/recurrent HCC was finally diagnosed depending on the follow-up imaging findings including further tumor growth or sustained iodized-oil accumulations in the hypervascular area on the hepatic arteriography with repeated TACE.
- In the benign conditions involving the perilesional hepatic parenchyma such as inflammatory, ischemic changes, or pseudolesions. The perilesional abnormal signal intensity area should disappear or decrease in size on MRI in 3 months follow-up.

3. Results

- Twenty-one out of the fifty patients had local tumor recurrence (Figs. 1 and 3).
- The size of chemoembolized lesions ranged from 1.5 to 8.5 cm. the maximum, minimum, mean and standard deviation of both malignant and benign groups are illustrated in Table 1.
- Among the 50 patients included in our study, 32% of lesions showed heterogenous signal intensity and 10% of the benign group lesions exhibited high T2 signal intensity that makes an assessment of HCC necrosis after TACE based on precontrast sequences signal intensity a conflict issue (Figs. 2, 4 and 5).
- In 86% of benign conditions the lesion border was circular compared to 52.3% of residual lesions.

Dynamic MRI had a sensitivity of 90.5%, a specificity of 96.6%, a positive predictive value of 95%, a negative predictive value of 93.3% and an overall agreement of 94% compared to 66.7%, 72.4%, 63.6%, 75% and 70% respectively in diffusion weighted imaging. If we regarded the scale 2 as a positive interpretation, the overall sensitivity of diffusion weighted imaging increased from 66.7% to 100% while the specificity decreased from 72.4% to 65.5% (Table 2).

- Regarding the pattern of diffusion restriction, 76.2% of true positive cases seen with diffusion weighted imaging exhibited focal peripheral nodular restriction, meanwhile 60% of the false positive cases exhibited intralesional heterogeneous restriction (Figs. 3 and 5)

Table 1 Represents the various maximum diameters of the tumors in cm.

Malignant	Benign	Dimension
1.7	1.5	Minimum
6	8.5	Maximum
3.52 ± 1.30	3.8 ± 1.90	Mean ± SD

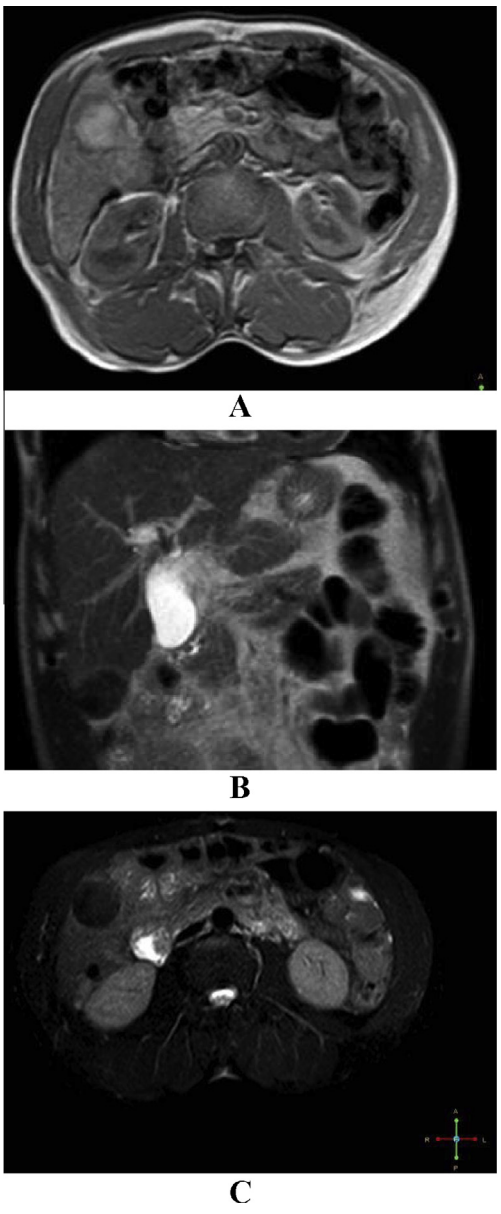

Fig. 2 Typical signal pattern of chemoembolized HCC. (A) Axial T1 FFE showing the typical high signal intensity of the right hepatic lobe (segment VI) chemoembolized HCC. (B) Coronal T2 TSE of the same patient showing the typical low signal intensity of the right hepatic lobe (segment VI) chemoembolized HCC. (C) Axial SPIR of the same patient showing the typical low signal intensity of the right hepatic lobe (segment VI) chemoembolized HCC.

- The difference between the malignant and benign groups ADC variables was statistically significant with a P value of 0.006.
- The ROC curve (Fig. 6) was obtained by plotting ADC variables at different cut off values. A statistical software estimated the area under the curve to be $C = 0.728$ with SE = 0.075 and 95% CI from 0.582 to 0.874.
- It seems from the ROC that the ADC variable is a fair indicator to differentiate marginal recurrence of HCC from perilesional benign lesions. The best cut off value that maximizes (sensitivity and specificity) is 1.26 mm^2/s. At this ADC value, the sensitivity is 95% and specificity is 59% (1−specificity = 0. 41)

4. Discussion

MRI provides anatomic details, as well as functional and molecular parameters for the assessment of the response of HCC to treatment. Authors stated that the successful tumoral treatment after TACE results in diminished blood supply with subsequent diminished tissue fluid. Thus the typical post treatment appearance is high signal intensity on T1-weighted images and low signal intensity on T2-weighted images (11–13).

Among the 50 patients included in our study, about 32% of lesions showed heterogenous signal intensity that makes an assessment of HCC necrosis after TACE based on precontrast sequences signal intensity a conflict issue. Also, it was reported that T2 hyperintensity not only represents residual tumor but also could represent hemorrhage, liquefactive necrosis, or inflammatory infiltrate (1). Therefore, it was difficult to assess the viable HCC tumors after TACE by conventional spin echo imaging. In our study 10% of the benign group lesions exhibited high T2 signal intensity.

Contrast-enhanced MRI is sensitive to therapy-related changes in blood volume and vascular permeability which may be associated with tumor angiogenesis (8). Braga et al. (12) stated that Dynamic MRI for unsuccessful TACE treatment shows focal enhanced regions admixed within non enhancing necrotic areas.

However, it was mentioned that the perilesional hypervascularity depicted by dynamic MRI is not specific only for the recurrent lesions but also occurs in benign conditions as a result of adjacent inflammation or other non tumorous arterioportal shunts, including direct arterioportal fistula or decreased portal venous flow related to iatrogenically induced portal tract injuries in the territory of selective TACE (14,1).

It was stated that benign conditions should show a perilesional rind-like contour and hyperintensity on delayed phase postcontrast images, meanwhile the residual lesions have more nodular contour and washout of the contrast medium on the delayed phase (15,16).

In the experience of Kim et al. (17) image subtraction was helpful for the assessment of the therapeutic efficacy for HCC by TACE in HCCs, which makes the depiction of tumor enhancement difficult on post-contrast T1-weighted images. Accordingly, to accurately assess tumor enhancement, we used the image subtraction techniques as well as color mapping images.

In our study, we had relatively lower sensitivity of dynamic MRI compared to other studies as we had two cases in which inappropriate breath holding led to motion artifact with subsequent false interpretation by the viewer. We had also one false positive case due to misinterpretation of a perilesional arterioportal shunt.

Diffusion-weighted imaging gives an insight about water content within a tumor and the degree of its viability. The viable tumor cells have intact membranes that cause restricted diffusion whereas necrotic tumors have increased water diffusion due to disruption of the cell membrane (18,19).

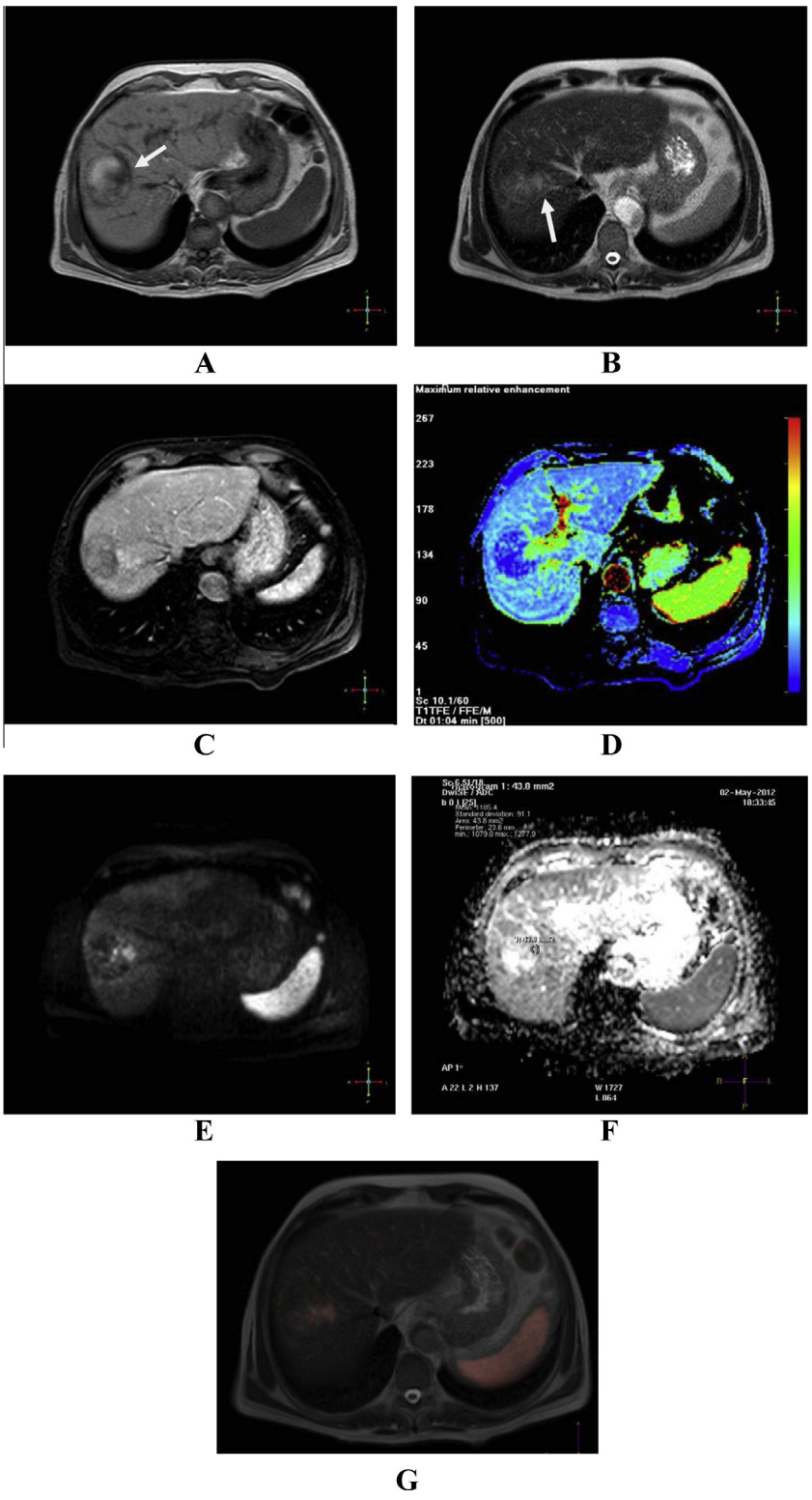

Fig. 3 Residual HCC. (A) Axial T1 FFE of 45 year old male with hepatitis C showing heterogenous predominantly high signal intensity of the right hepatic lobe chemo- embolized HCC. Note the medial hypointense medial portion of the lesion (arrowed). (B) Axial T2 TSE of the same patient showing heterogenous signal intensity of the lesion with high signal intensity of its medial portion (arrowed). (C and D) axial early arterial phase of T1 THRIVE and corresponding maximum relative enhancement of the same patient showing early arterial enhancement of the medial residual portion. (E and F) Diffusion weighted imaging (*b* value 1000) and the corresponding ADC showing restricted diffusion of the medial portion of the lesion with ADC value of 1.18 ± 0.91.Note the nodular pattern of diffusion restriction. (G) Fusion image showing overlap between the high signal intensity medial portion of the lesion on T2 WIs and the restriction seen on diffusion images (*b* value 1000).

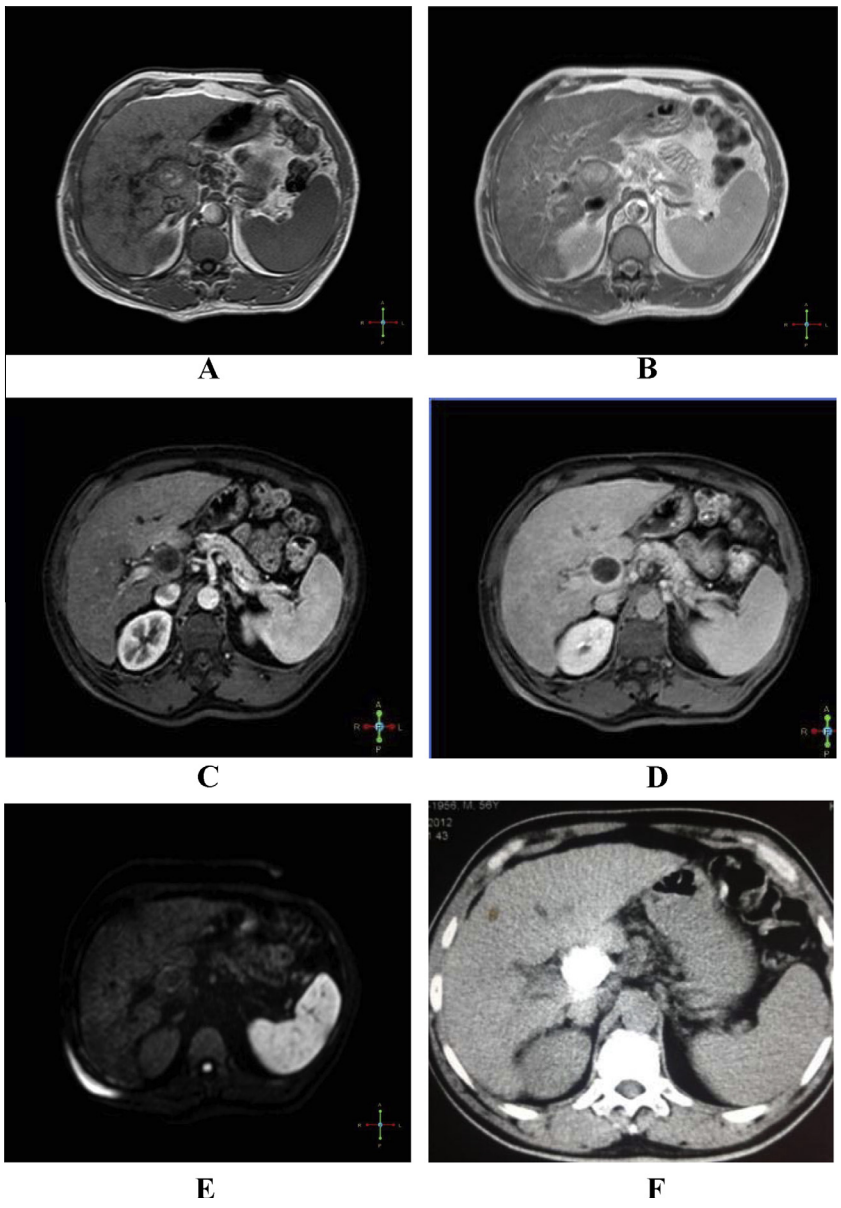

Fig. 4 complete ablation of caudate lobe HCC. (A) Axial T1 FFE of 56 year old male showing heterogenous signal intensity of a caudate lobe chemo-embolized HCC. (B) Axial T2 SSh of the same patient showing central core of high signal intensity with peripheral rim of low signal intensity. (C) Axial early arterial phase of T1 THRIVE showing faint peripheral rim enhancement. (D) Axial post contrast T1FFE showing progressive increase of the uniform peripheral rim of enhancement. (E) Axial respiratory triggered diffusion weighted image (*b* value 1000) showing faint uniform peripheral rim of high signal intensity. (F) Non contrast CT of the same patient showing dense lipiodol uptake by the tumor.

Many studies confirmed that individuals with HCC who responded to chemoembolization treatment showed a significant rise in the ADC values after treatment (20–22,6). Interestingly, a significant rise in the ADC values following TACE in patients with HCC could be detected as early as 12–24 h after therapy in patients who were subsequently defined as responders by RECIST criteria (23).

Practically, however, Yu et al. stated that it is more important to know whether the procedure was complete or incomplete rather than calculating ADC values before and after the procedure. They measured the ADC value to differentiate between the marginal recurrences of HCC from perilesional benign conditions. They found that the ADC values varied widely for the nontumorous lesions and grossly overlapped with the viable tumor portion making it impossible to determine any cutoff points.

They reported that DWI increased the sensitivity for the detection of post TACE residual HCC with increased false positives. Thus, the decreased specificity compromised the increased sensitivity gained by DWI and decreased the overall diagnostic accuracy. They referred the increase in false positive findings to perilesional parenchymal insults that showed sustained hyperintensity on DWI with increasing *b* factors. They demonstrated that hypercellularity intermingled with a fibrotic

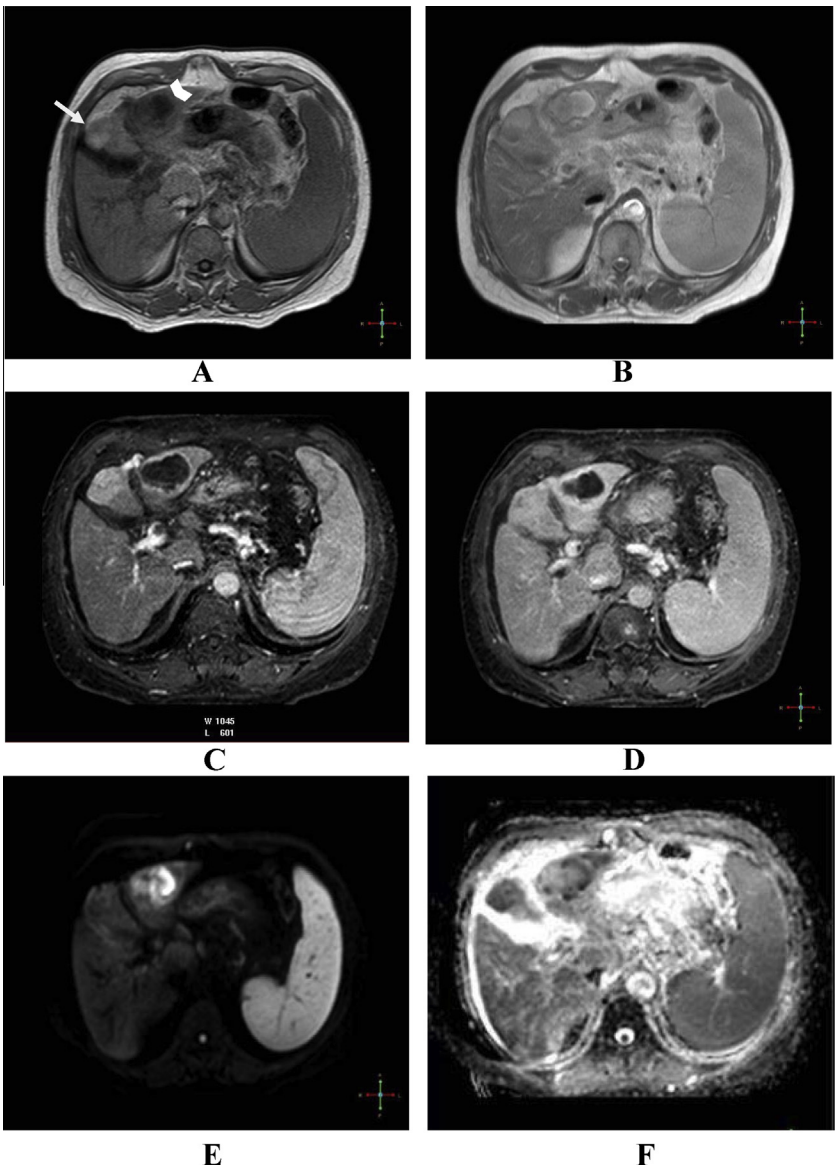

Fig. 5 Complete ablation of HCC with newly detected HCC nodule. (A) Axial T1 FFE of 60 year old male shows heterogenous signal intensity of a left hepatic lobe (segment II) chemo-embolized HCC (arrowhead). Note the left hepatic lobe (Segment IVb) high signal intensity dysplastic nodule (arrowed) with faint hypointensity of its medial portion(nodule with nodule sign). (B) Axial T2 ssh of the same patient showing heterogenous signal intensity of the left hepatic lobe (segment II) chemo-embolized HCC (arrowhead). Note the reversal of signal intensity of the segment IVb lesion with the dysplastic nodule exhibiting low signal compared to the high signal of the medial HCC nodule. (C) Axial early arterial phase of T1 THRIVE showing peripheral rim enhancement in segment II chemoembolized lesion. Note the heterogenous enhancement of the segment IVb focal lesion. (D) Axial delayed phase of T1 THRIVE showing progressive increase of the peripheral rim of enhancement of segment II chemoembolized lesion. Note the wash out of the medial HCC nodule of segment IVb lesion with near isointensity of the lateral dysplastic nodule. (E and F) Axial respiratory triggered diffusion weighted image (*b* value 1000) and the corresponding ADC showing heterogenous marked restriction of the chemoembolized HCC.

content in the inflammatory granulation tissue could cause restricted diffusion, resulting in sustained hyperintensity on DWI.

In our study, 10 false positive cases out of 50 patients were misdiagnosed on diffusion weighted imaging. When we reviewed the corresponding pattern of diffusion restriction, 76.2% of true positive cases exhibited focal peripheral nodular restriction, meanwhile 60% of the false positive cases exhibited intralesional heterogenous restriction (Fig. 6). So, we considered that the increase in false positive findings in our study is likely originating from intralesional hemorrhage or liquefactive necrosis that causes diffusion restriction. In the studies of Holtas et al., Tung et al., Batra et al. (24–26) sterile liquefactive necrosis and intracavitary microhaemorrhage are accepted to be the cause of hyperintensity in diffusion-weighted MR images of malignant necrotic lesions.

Our results are matching with those of yu et al. and Goshima et al. (27) showing dynamic contrast enhanced MRI to be

Table 2 Diagnostic indices (sensitivity, specificity, PPV, NPV and overall agreement) of dynamic and diffusion MRI in the studied group.

DWI (%)	Dynamic mri (%)	
100	90.5	Sensitivity
65.5	96.6	Specificity
67.7	95	PPV
100	93.3	NPV
80	94	Overall agreement

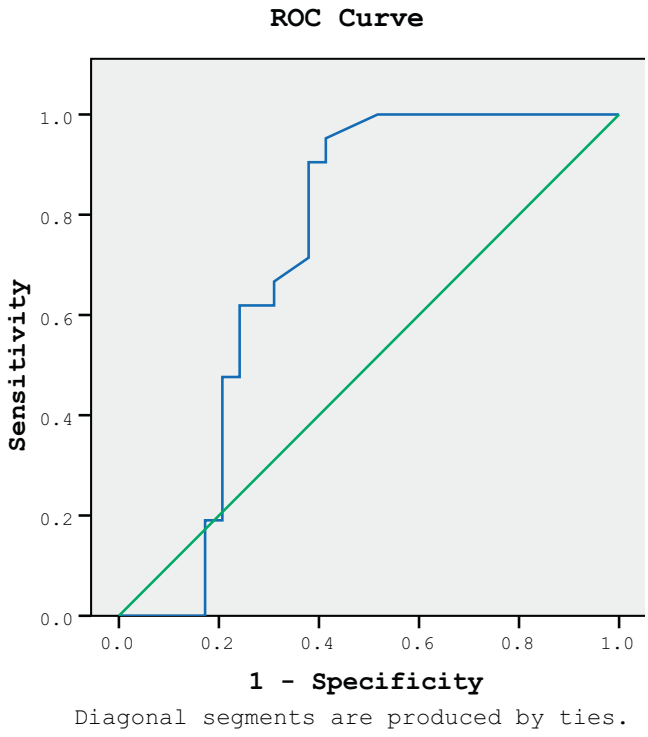

Fig. 6 Results of receiver operating curves for ADC values in distinguishing benign and malignant groups.

superior to diffusion weighted MRI in evaluating HCC response to treatment.

Diffusion weighted MRI has some advantages compared to dynamic MRI. First, contrast medium administration is not required, and the examination is obtained in a relatively short time. Second, the technique is easy to be repeated, allowing close follow-up during and after tumor treatment. Also, image post-processing is less time-consuming compared to dynamic contrast-enhanced MR imaging. At last, Diffusion-weighted MR imaging allows easy evaluation of the whole tumor. This is important because of the inhomogeneity that may occur within tumors (28).

In addition, respiratory triggered diffusion weighted images compensated the false results by the dynamic MRI in our patients who could not hold their breath adequately.

In our study, we had some diagnostic limitations. First, it was difficult to obtain pathologic confirmation in patients who underwent chemoembolization because all of these patients were not subjected to surgery. Second, lesions included in our study were larger than 1 cm in diameter and a few of them were located at the hepatic dome. The aforementioned factors could cause selection bias leading to increased sensitivity of diffusion weighted images, since hepatic lesions close to the diaphragm pose a challenge to DW-MRI evaluation, as they are more sensitive to motion, susceptibility artefacts, as well as artefacts arising from the heart.

In conclusion, in our study, we found that complementary dynamic and diffusion MRI achieve effective monitoring of tumor response to therapy.

Conflict of interest statement

None to declare.

Acknowledgments

The authors are grateful for Dr. Ashraf Omar head of HCC unit of the tropical department. They are also thankful for the assistant technical MRI team of the Kasr Al-Ainy Hospital for their technical contribution.

References

(1) Özkavukcu E, Haliloğlu N, Erden A. Post-treatment MRI findings of hepatocellular carcinoma. Diagn Interv Radiol 2009;15(2):111–20.
(2) Chen M, Li J, Zhang Y, Lu L, Zhang W, Yuan Y, et al. High-dose iodized oil transcatheter arterial chemoembolization for patients with large hepatocellular carcinoma. World J Gastroenterol 2002;8(1):74–8.
(3) Jang KM, Choi D, Lim HK, Lim JH, Lee JY, Lee WJ, et al. Depiction of viable tumor in hepatocellular carcinoma treated with transarterial chemoembolization multiphasic helical CT with review of previous serial CT images. Korean J Radiol 2005;6:153–60.
(4) Forner A, Ayuso C, Varela M, Rimola J, Hessheimer A, de Lope C, et al. Evaluation of tumor response after locoregional therapies in hepatocellular carcinoma are response evaluation criteria in solid tumors reliable? Cancer 2009;115(3):616–23.
(5) Takayasu K, Arii S, Matsuo N, Yoshikawa M, Ryu M, Takasaki K, et al. Comparison of CT findings with resected specimens after chemoembolization with iodized oil for hepatocellular carcinoma. AJR Am J Roentgenol 2000;175(3):699–704.
(6) Jiang ZX, Peng WJ, Li WT, Tang F, Liu SY, Qu XD, et al. Effect of *b* value on monitoring therapeutic response by diffusion-weighted imaging. World J Gastroenterol 2008;14(38):5893–9.
(7) Sorensen AG. Magnetic resonance as a cancer imaging biomarker. J Clin Oncol 2006;24(20):3274–81.
(8) Hamstra DA, Rehemtulla A, Ross BD. Diffusion magnetic resonance imaging a biomarker for treatment response in oncology. J Clin Oncol 2007;25(26):4104–9.
(9) Liapi E, Geschwind JF, Vossen JA, Buijs M, Georgiades CS, Bluemke DA, et al. Functional MRI evaluation of tumor response in patients with neuroendocrine hepatic metastasis treated with transcatheter arterial chemoembolization. AJR 2008;190(1):67–73.
(10) Buijs M, Vossen JA, Hong K, Georgiades CS, Geschwind JF, Kamel IR. Chemoembolization of hepatic metastases from ocular melanoma assessment of response with contrast-enhanced and diffusion weighted MRI. AJR Am J Roentgenol 2008;191(1):285–9.

(11) Leea C, Bragac L, Camposa R, Semelka R. Hepatic tumor response evaluation by MRI. NMR Biomed 2011;24(6):721–33, doi.10.1002/nbm.1637. Epub 2010 Dec 12..
(12) Braga L, Guller U, Semelka RC. Pre-, peri-, and posttreatment imaging of liver lesions. Radiol Clin North Am 2005;43(5):915–27.
(13) Semelka RC, Worawattanakul S, Mauro MA, Bernard SA, Cance WG. Malignant hepatic tumors changes on MRI after hepatic arterial chemoembolization – preliminary findings. J Magn Reson Imaging 1998;8(1):48–56.
(14) Braga L, Armao D, Azzazi ME, Semelka RC. Liver. In: Semelka RC, editor. Abdominal-Pelvic MRI. Hoboken, NJ: Wiley-Blackwell; 2010. p. 445–54.
(15) Hwang SH, Yu JS, Chung J, Chung JJ, Kim JH, Kim KW. Transient hepatic attenuation difference (THAD) following transcatheter arterial chemoembolization for hepatic malignancy changes on serial CT examinations. Eur Radiol 2008;18(8):1596–603.
(16) Yu JS, Kim JH, Chung JJ, Kim KW. Added value of diffusion-weighted imaging in the MRI assessment of perilesional tumor recurrence after chemoembolization of hepatocellular carcinomas. J Magn Reson Imaging 2009;30(1):153–60.
(17) Kim S, Mannelli L, Hajdu CH, Babb JS, Clark TW, Hecht EM, et al. Hepatocellular carcinoma assessment of response to transarterial chemoembolization with image subtraction. J Magn Reson Imaging 2010;31(2):348–55.
(18) Qayyum A. Diffusion-weighted imaging in the abdomen and pelvis. Concepts Appl Radiograph 2009;29(6):1797–810.
(19) Geschwind JF, Artemov D, Abraham S, Omdal D, Huncharek MS, McGee C, et al. Chemoembolization of liver tumor in a rabbit model assessment of tumor cell death with diffusion-weighted MR imaging and histologic analysis. J Vasc Interv Radiol 2000;11(10):1245–55.
(20) Kamel IR, Bluemke DA, Ramsey D, Abusedera M, Torbenson M, Eng J, et al. Role of diffusion-weighted imaging in estimating tumor necrosis after chemoembolization of hepatocellular carcinoma. AJR Am J Roentgenol 2003;181(3):708–10.
(21) Kamel IR, Bluemke DA, Eng J, Liapi E, Messersmith W, Reyes DK, et al. The role of functional mr imaging in the assessment of tumor response after chemoembolization in patients with hepatocellular carcinoma. J Vasc Interv Radiol 2006 Mar;17(3):505–12.
(22) Mannelli L, Kim S, Hajdu CH, Babb JS, Clark TW, Taouli B, et al. Assessment of tumor necrosis of hepatocellular carcinoma after chemoembolization diffusion-weighted and contrast-enhanced MRI with histopathologic correlation of the explanted liver. AJR Am J Roentgenol 2009;193(4):1044–52.
(23) Kamel IR, Liapi E, Reyes DK, Zahurak M, Bluemke DA, Geschwind JF. Unresectable hepatocellular carcinoma. Serial early vascular and cellular changes after transarterial chemoembolization as detected with MR imaging. Radiology 2009;250(2):466–73.
(24) Holtas S, Geijer B, Stromblad LG, Maly-Sundgren P, Burtscher IM. A ring-enhancing metastasis with central high signal on diffusion-weighted imaging and low apparent diffusion coefficients. Neuroradiology 2000;42(11):824–7.
(25) Tung GA, Evangelista P, Rogg JM, Duncan JA. Diffusion-weighted MR imaging of rim enhancing brain masses.is markedly decreased water diffusion specific for brain abscess? AJR Am J Roentgenol 2001;177(3):709–12.
(26) Batra A, Tripathi RP. Atypical diffusion-weighted magnetic resonance findings in glioblastoma multiforme. Australas Radiol 2004;48(3):388–91.
(27) Goshima S, Kanematsu M, Kondo H, Yokoyama R, Tsuge Y, Shiratori Y, et al. Evaluating local hepatocellular carcinoma recurrence post- transcatheter arterial chemoembolization is diffusion-weighted MRI reli- able as an indicator? J Magn Reson Imaging 2008;27(4):834–9.
(28) Thoeny HC, De Keyzer F, Chen F, Ni Y, Landuyt W, Verbeken EK, et al. Diffusion- weighted MR imaging in monitoring the effect of a vascular targeting agent on rhabdomyosarcoma in rats. Radiology 2005;234(3):756–64.